HD207897 B: A DENSE SUB-NEPTUNE TRANSITING A NEARBY AND BRIGHT K-TYPE STAR

N.Heidari[1,2 3], I. Boisse[3], SOPHIE team and others

Abstract. We present the discovery and characterization of a transiting sub-Neptune orbiting with a 16.20-day period around a nearby (28 pc) and bright (V= 8.37) K0V star HD207897 (TOI-1611). This discovery is based on photometric measurements from the Transiting Exoplanet Survey Satellite (TESS) mission and radial velocity (RV) observations from the SOPHIE, Automated Planet Finder (APF) and HIRES high precision spectrographs. We used EXOFASTv2 for simultaneously modeling the parameters of the planet and its host star, combining photometry and RVs data to determine the planetary system parameters. We show that the planet has a radius of 2.50 ± 0.08 R_E and a mass of either 14.4 ± 1.6 M_E or 15.9 ± 1.6 M_E with nearly equal probability; the two solutions correspond to two possibilities for the stellar activity period. Hence, the density is either 5.1 ± 0.7 g cm^{-3} or $5.5^{+0.8}_{-0.7}$ g cm^{-3}, making it one of the relatively rare dense sub-Neptunes. The existence of such a dense planet at only 0.12 AU from its host star is unusual in the currently observed sub-Neptune ($2 < R_E < 4$) population. The most likely scenario is that this planet has migrated to its current position.

Keywords: planets and satellites: detection, techniques: photometric, techniques: radial velocities

1 Introduction

The NASA *Kepler* and *TESS* Mission have discovered a large number of planets of intermediate size, with radii between Earth and Neptune, also known as sub-Neptunes. Since the size of planets is directly dependent on physical mechanisms in formation and evolution, the absence of sub-Neptunes in our solar system and their abundance among exoplanet population has raised numerous fundamental questions.

Here, we announce the detection and characterization of a sub-Neptune orbiting a bright (V=8.4) K0 star using TESS photometry data and SOPHIE, APF, and HIRES RVs.

2 Observations

2.1 Photometry

TESS observations of HD207897 were taken on five sectors divided into two continuous periods from sectors 18-20 and 25-26, with a total time span of 131 days. After observations of sector 18 were completed, the MIT's Quick Look pipeline detected the signature of two transits of HD207897 b at a period of 16.20 d, and an alert was issued 19 December 2019 by the TESS Science Office. No transits occurred during sector 19 as the sole transit fell in the data gap between the two orbits. After observations of sector 20 were downlinked, the Science Processing Operations Center (SPOC; Jenkins et al. 2016) at NASA Ames Research Center conducted a transit search detected two transits of HD207897 b at a signal-to-noise ratio (S/N) of 23.3. Two additional transits were observed and detected in sector 25, and one more occurred during sector 26. A multi-sector search of sectors 18-26 by the SPOC detected 7 transit events of HD207897 b in total, at an S/N of 34.3 and an average depth of 913.7±21.1 ppm.

[1] Department of Physics, Shahid Beheshti University, Tehran, Iran.
[2] Laboratoire J.-L. Lagrange, Observatoire de la Côte d'Azur (OCA), Université de Nice-Sophia Antipolis (UNS), CNRS, Campus Valrose, 06108 Nice Cedex 2, France.
[3] Aix Marseille Univ, CNRS, CNES, LAM, Marseille, France.

We used 2-minutes photometry data which was extracted with the Pre-search Data Conditioned Simple Aperture Photometry (PDC-SAP) pipeline provided by the TESS team. The normalized and detrended light curve is shown in Figure 1.

To look for any periodic signals in the data, we used the transit-least-squares (TLS) algorithm (Hippke & Heller 2019). We found a prominent periodic signal occurring every 16.20 d with a S/N of 43, with false alarm probability (FAP) below 0.01 %.

2.2 High-resolution spectroscopy

HD207897 had been monitored between 2012 to 2020 by the SOPHIE spectrograph (Perruchot et al. 2008). The observations were performed using high-resolution mode with a simultaneous Thorium-Argon (Th-Ar) or Fabry perot calibration lamp, allowing us to monitor the instrumental drift. We collected 68 spectra with an exposure time ranging from 1000 to 1500 s and a median signal-to-noise ratio (S/N) of 97.7 per pixel at 550 nm. The mean RVs uncertainty is also 1.7 m s^{-1}.

We also observed this satr using the Keck I telescope and HIRES spectrometer (Vogt 1994) from 2003, and additional RVs were collected for eleven months beginning on 2020 Jan 21. Thirty-seven RVs were collected using the B5 decker (0.87" x 5.0") resulting in a resolution of 50,000. The median exposure time was 231 s, an average signal-to-noise ratio per pixel of 220, and internal uncertainty of 1.04 m/s.

Morover, from the summit of Mt. Hamilton at Lick Observatory, we collected 23 more RVs of HD207897 using the Levy Spectrograph on the APF from 2 Jun 2020 until 28 Feb 2021. Twenty-three RVs were collected having a median exposure time of 1200s, a signal to noise per pixel of 86, and internal uncertainty of 3.0 m/s. With resolution of 100,000, this slit-fed spectrograph uses the iodine-cell technique to calculate RVs descended from.

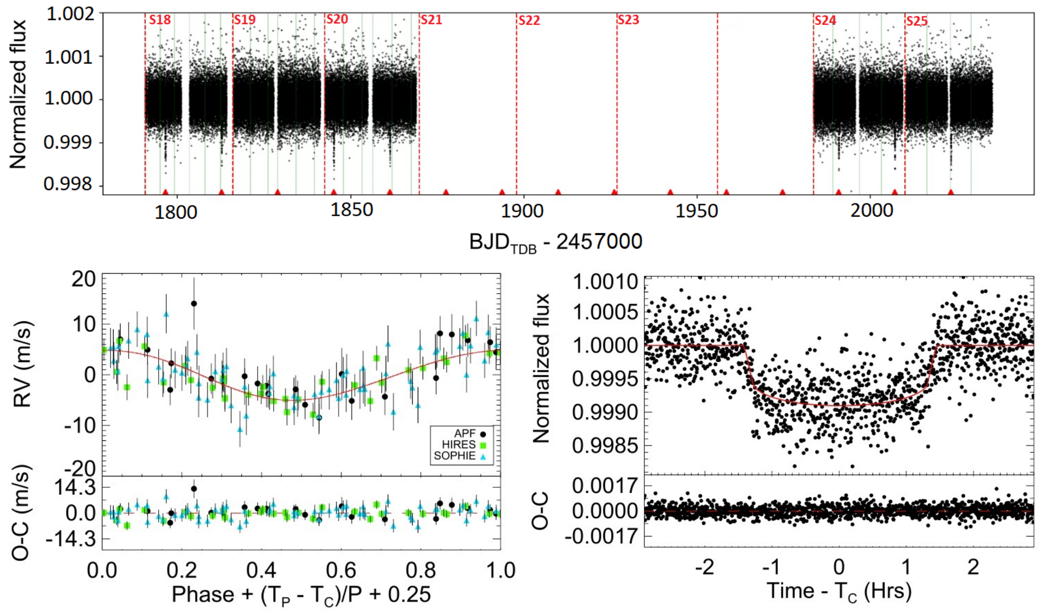

Fig. 1. Top: The Full PDC-SAP (2-minute) TESS light curve after detrending. **Left:** Phase-folded SOPHIE, APF, and HIRES RVs of HD207897 b at the period of 16.20 d. **Right:** TESS Phase-folded light curve.

3 Radial velocity data analysis

The data are extract by Doppler shifted method. After removing a drift, we investigated the footprints of the planet by searching for periodic signals. To do so we used the Data and Analysis Center for Exoplanets (DACE, Delisle et al. 2016) web platform and computed periodograms for RVs (Fig. 2).

The RVs periodogram displays a clear peak at 16.20 d with a value below 0.1 % false alarm probability (Baluev 2008). Moreover, there is no corresponding peak in the periodogram of activity indicators, which shows that this periodic signal is likely due to a planet and not due to stellar activity, Figure 2.

Table 1. Median values and 68% confidence interval for HD207897 b and its host star.

Parameter	Units	Activity on 35.9 d (Prob. = 46%)	Activity on 37.6 d (Prob. = 54%)
M_*	Mass (M_{sun})	$0.801^{+0.036}_{-0.031}$	$0.800^{+0.036}_{-0.030}$
R_*	Radius (R_{sun})	$0.779^{+0.019}_{-0.018}$	$0.779^{+0.019}_{-0.018}$
P	Period (days)	16.202157 ± 0.000085	$16.202159^{+0.000085}_{-0.000083}$
ρ_P	Density (cgs)	$\mathbf{5.52}^{+0.82}_{-0.73}$	$\mathbf{5.05}^{+0.77}_{-0.69}$
R_P	Radius ($R_\oplus$)	$2.505^{+0.081}_{-0.077}$	$2.501^{+0.082}_{-0.078}$
M_P ...	Mass ($M_\oplus$)	**15.9**$\pm$1.6	**14.4**$\pm$1.6
a	Semi-major axis (AU)	$0.1164^{+0.0017}_{-0.0015}$	$0.1163^{+0.0017}_{-0.0015}$

Moreover of the planet signal, there is also two signals at 35.9 d and 37.6 d in RV residuals. The estimated rotational period of star using extracted $\log(R'_{HK})$ from SOPHIE spectra, is 37 ± 7 d. Also, there is a peak at 36 d in periodogram of CRX activity indicator. So, it is likely the signals at 35.9 d and 37.6 d are due to stellar rotational period.

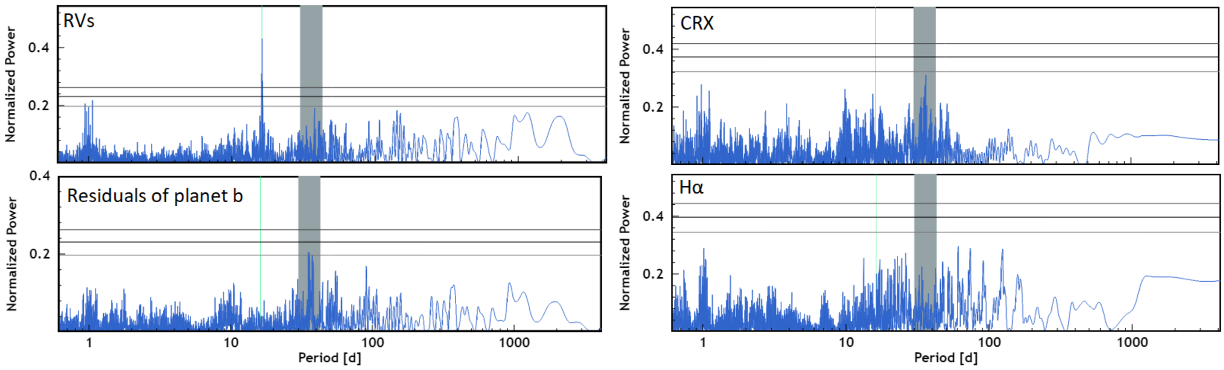

Fig. 2. Left: RVs and residual of RVs after Keplerian fit on 16.20 d. **Right:** CRX and $H\alpha$ index. The cyan vertical line marks the position of highest peak at RVs periodogram at 16.20 d. Horizontal lines indicate 0.1, 1, 10 % FAP level, from top to bottom, respectively. Also, the grey vertical strip is highlighting the position of the estimated rotational period of star.

4 Joint modeling of RV and photometry

To explore all the parameters of the system, including both the host star and the planet, we modeled simultaneous and self-consistent the photometric observations and RV measurements using the Fast Exoplanetary fitting package (EXOFASTv2, Eastman et al. 2019).

As we showed in Sect. 3, the signals at 35.9 and 37.6 d are likely to be due to the stellar rotation periods. Since these signals affect slightly the mass estimate of the planet, we considered them as an additional keplerian fit in our global analysis. We did not fix the period and let EXOFASTv2 find the best activity period between 35.9 and 37.6 d signals. After EXOFASTv2 converged, we saw a bimodality in the posterior distribution for the stellar activity periods, so we present the final median posterior distributions values of both the most probable solutions in Table 1. We also report their calculated probabilities based on the area of the posterior distributions. The probability of the most likely values is 54% and the less likely values are 46%.

5 Discussion and Summary

In this paper, we detected and characterized a sub-Neptune orbiting around HD207897, with a period of 16.202161 ± 0.000083 d, using TESS photometry data along with SOPHIE, HIRES, and APF RVs observations. We found the planet has a mass of 14.4 ± 1.6 M_E with probability of 56 % (or 15.9 ± 1.6 M_E with probability of 46 % based on bimodal results of stellar activity period) and a radius of 2.5 ± 0.08 R_E, which translates into a high density of 5.1 ± 0.7 g cm^{-3} (or $5.5^{+0.8}_{-0.7}$ g cm^{-3}). We used the same mass and radii bounds as Otegi et al.

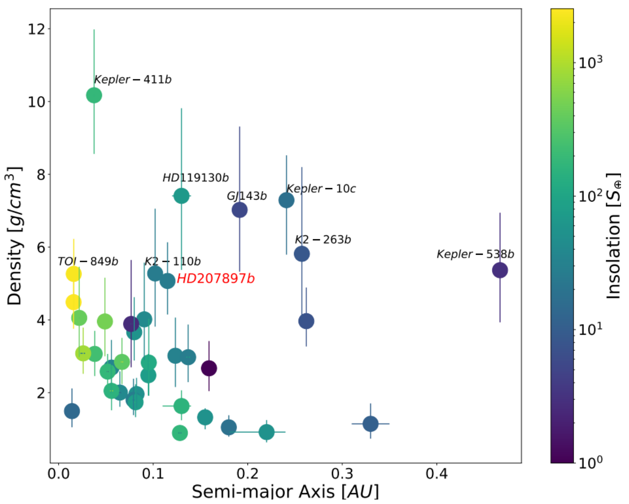

Fig. 3. The density-semi major axis diagram for HD207897 b and other sub-Neptune sized planets ($2 < R_{\rm E} < 4$) with known semi-major axis, luminosity and accurate mass and radius (Otegi et al. 2020). Dots are colored with planet insolation in Earth unit.

(2020) on NASA Exoplanet Data Archive* (December 5th, 2020) and plotted in Fig 3, all the sub-Neptune sized planets ($2 < R/R_{\rm E} < 4$) with semi-major axis and luminosity determined.

How can HD207897 b and other similar planets with such a high density exist at a close distance from their host star? One possibility could be that the planet has lost most of its volatile elements by evaporation, but for the case of HD207897 b with an orbital period of 16.20 d and receiving an incident flux of F=26.3 $F_{\rm E}$ it is not a satisfactory answer. Indeed, even if we consider an extreme evaporation process (Lecavelier Des Étangs 2007), the mass-loss of the planet would be just 0.1 $M_{\rm E}$ during the entire lifetime of the star, which cannot account for its high density. HD207897 b is unlikely to have formed in situ. According to Schlichting (2014) the maximum isolation mass that can form at a distance of a = 0.12 AU is only $\sim$ 0.06 $M_{\rm E}$, assuming the minimum mass solar nebula (MMSN); a disk surface density $\sim$ 41 times larger than the solar nebula would be required to form a planet as massive as HD207897 b at this distance. Two possible scenarios can however be considered, both consistent with the MMSN: either the material from the outer region migrated and formed the planet HD207897 b or the formation of HD207897 b occurred far out of the disc and the planet subsequently migrated to its current location. The second scenario could have been triggered by another planet in this system. The hint of long-term trend on RVs allows for the presence of another planet. The high occurrence rate of long-period giant planets ($mass > 0.3 M_{\rm J}$) in the systems harboring small planets (planets with mass/radius between Earth and Neptune) (Schlecker et al. 2020) can also support such a scenario.

References

Baluev, R. V. 2008, Monthly Notices of the Royal Astronomical Society, 385, 1279

Delisle, J.-B., Ségransan, D., Buchschacher, N., & Alesina, F. 2016, Astronomy & Astrophysics, 590, A134

Eastman, J. D., Rodriguez, J. E., Agol, E., et al. 2019, arXiv preprint arXiv:1907.09480

Hippke, M. & Heller, R. 2019, A&A, 623, A39

Jenkins, J. M., Twicken, J. D., McCauliff, S., et al. 2016, in Software and Cyberinfrastructure for Astronomy IV, Vol. 9913, International Society for Optics and Photonics, 99133E

Lecavelier Des Étangs, A. 2007, Astronomy & Astrophysics, 461, 1185

Otegi, J., Bouchy, F., & Helled, R. 2020, Astronomy & Astrophysics, 634, A43

Perruchot, S., Kohler, D., Bouchy, F., et al. 2008, 7014, 70140J

Schlecker, M., Mordasini, C., Emsenhuber, A., et al. 2020, Astronomy & Astrophysics

Schlichting, H. E. 2014, The Astrophysical Journal Letters, 795, L15

*https://exoplanetarchive.ipac.caltech.edu/